Available online at www.sciencedirect.com

ScienceDirect

IFAC PapersOnLine 50-1 (2017) 10913–10917

Tracking Control of a Monolithic Piezoelectric Nanopositioning Stage using an Integrated Sensor.

Meysam Omidbeike * **Yik R. Teo** * **Yuen K. Yong** * **Andrew J. Fleming** *

* *Precision Mechatronics Lab, The University of Newcastle, Callaghan, NSW, 2308, Australia (e-mail: meysam.omidbeike@uon.edu.au).*

Abstract: This article describes a method for tracking control of monolithic nanopositioning systems using integrated piezoelectric sensors. The monolithic nanopositioner is constructed from a single sheet of piezoelectric material where a set of flexures are used for actuation and guidance, and another set are used for position sensing. This arrangement is shown to be highly sensitive to in-plane motion (in the x- and y-axis) and insensitive to vertical motion, which is ideal for position tracking control. The foremost difficulty with piezoelectric sensors is their low-frequency high-pass response. In this article, a simple estimator circuit is used to allow the direct application of integral tracking control. Although the system operates in open-loop at DC, dynamic command signals such as scanning trajectories are accurately tracked. Experimental results show significant improvements in linearity and positioning error.

Keywords: Nanopositioner, Tracking Control, Piezoelectric

1. INTRODUCTION

Nanopositioning systems provide sub-atomic positioning resolution in applications such as scanning probe microscopes (Fleming and Leang, 2014; Salapaka and Salapaka, 2008; Abramovitch et al., 2007), nanofabrication (Mishra et al., 2007), precision optics (Hassen et al., 2009) and data storage (Sebastian et al., 2008).

A new class of monolithic nanopositioning design was recently reported where an XY nanopositioner was constructed from a single sheet of piezoelectric material (Fleming and Leang, 2014). Active flexures were formed by removing parts of the sheet to provide both actuation and motion guidance. In addition, it is possible to use the flexures as sensors. These piezoelectric strain sensors have a wide sensing bandwidth, low noise at high frequencies and high sensitivity (Sirohi and Chopra, 2000). Of all the properties, the most notable advantage is the high sensitivity to in-plane motions while maintaining low sensitivity to out of plane motion. As a result, the sensor is an ideal variable for feedback control (Fleming and Leang, 2010).

Piezoelectric sensors have excellent AC properties, however, their capacitive source impedance imposes a first-order high-pass response at low frequencies. Due to their high-pass characteristic, piezoelectric sensors are mainly used in damping and vibration control (Kuiper and Schitter, 2010; Fleming, 2010)but not in tracking control. The high-pass characteristic causes instability if enclosed in an integral control loop. A common approach to overcome this is the low-frequency bypass techniques (Fleming, 2010; Yong et al., 2011, 2013). In this method, the low-frequency component of the sensor output is replaced with either an estimate from the input actuation voltage or

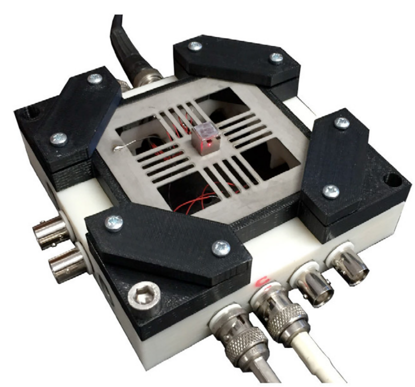

Fig. 1. Nanopositioner mounted on a base.

an auxiliary DC sensor measurement. A pair of complementary filters are used to combine the low-frequency estimate and the high-frequency measurement. However, the complementary filters introduce an extra pole which must have a significant higher cut-off frequency than that of the buffered piezoelectric sensor, which can result in a long settling time.

In this article, the high-pass characteristic of the sensor is compensated by using the impedance of the piezoelectric sensor as a circuit component in a complimentary filter. This approach provides immunity to variations in the piezoelectric capacitance since the low- and high-pass cut-off frequencies are now matched. The proposed technique is demonstrated on the monolithic XY nanopositioning device reported in Fleming et al. (2016).

This article is organized as follow, the experimental set up is discussed in Section 2. In Section 3, the characteristics

Peer review under responsibility of International Federation of Automatic Control.
10.1016/j.ifacol.2017.08.2455

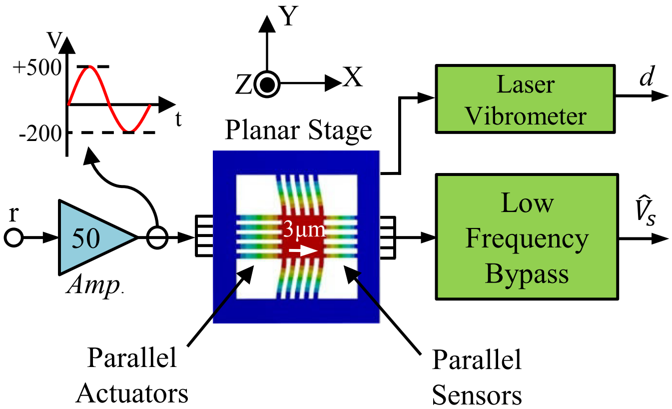

Fig. 2. Experimental configuration of nanopositioner

of piezoelectric sensor are discussed. The low frequency bypass technique is introduced in Section 4. The feedback control design and tracking performance is discussed in Section 5.

2. EXPERIMENTAL SET UP

The piezo-stage was fabricated from a monolithic square sheet of PZT-5A ceramic with dimensions 72.3 mm × 72.3 mm × 0.5 mm (Fleming et al., 2016). The sheet has Nickel electrodes sputter coated to a thickness of 5 μm on each side. The nanopositioner is mounted on an insulating base as shown in Fig. 1. The full range of the stage when driven in a push-pull configuration is 6.5 μm.

The experimental configuration of a single-freedom nanopositioning stage is shown in Fig. 2. In this application, the flexures on one side are used as actuators and the flexures on the opposite side as sensors. The actuators are driven in parallel with −200 V to 500 V where the corresponding travel range is 3 μm. The displacement and frequency responses of the system are recorded using a Polytec MSA-500 laser vibrometer. The open-loop frequency response of the system in the X-axis and the cross-coupling responses in the Y- and Z-axis are illustrated in Fig. 5.

3. PIEZOELECTRIC SENSOR CHARACTERISTIC

In this experiment the integrated piezoelectric sensor is used to estimate the position of the platform. Fig. 3 shows the sensor output voltage when the positioner is driven at full range. The piezoelectric strain sensor consists of five parallel beams with the measured sensitivity of 3.63 V/μm and a capacitance of 5.4 nF. The foremost limitation of piezoelectric sensors is the high-pass characteristic due to the combination of the sensor's internal capacitance and the input impedance of the conditioning electronics. As a result, the piezoelectric sensor can only be used at frequencies above the cut-off frequency of the high-pass filter. The transfer function is

$$F_{HP} = \frac{V_s}{v_a} = \frac{s}{s+\omega_c}, \qquad \omega_c = \frac{1}{2\pi C_p R_{in}} \text{ Hz} \tag{1}$$

where v_a is the actuation voltage, V_S is the sensor output voltage, ω_c is the cut-off frequency and R_{in} is the input impedance of the electronics connected to the sensor.

To demonstrating the effect of the high-pass filter on integral tracking control, the sensor voltage V_s is used as a feedback variable for tracking control. Fig. 4 shows a block diagram of the control system where $C = \alpha/s$ is a integral controller with gain α, the transfer function from the control signal u to the sensor voltage V_s is $G_{V_s u}$ and F_{HP} represent the high-pass characteristic of the sensor.

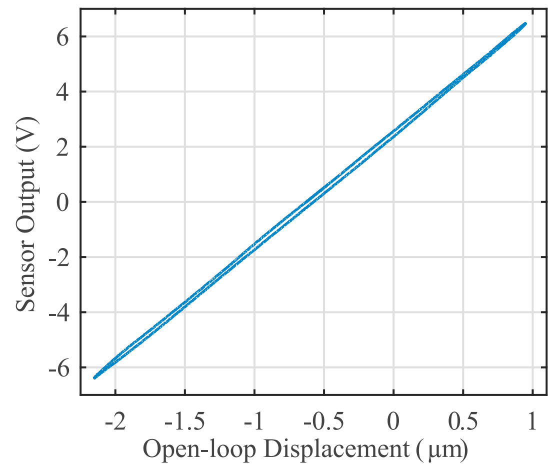

Fig. 3. The full range open loop displacement versus the sensor voltage output.

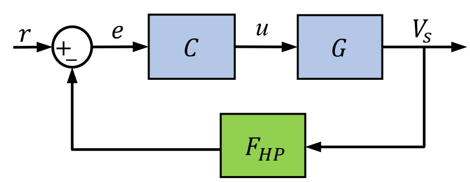

Fig. 4. Block diagram of an integral tracking loop with high-pass filtered output.

The sensitivity function for this system from r to V_s is,

$$\frac{V_s}{r} = \frac{G_{V_s u} C}{1 + G_{V_s u} C F_{HP}}, \tag{2}$$

If $G_{V_s} u(s)$ is parameterized as

$$G_{V_s} u(s) = \frac{N(s)}{D(s)},$$

the sensitivity function (2) simplifies to

$$\frac{V_s}{r} = \frac{1}{s} \frac{\alpha N(s)(s+\omega_c)}{(D(s)(s+\omega_c) + \alpha N(s)))}, \tag{3}$$

where ω_c is cut off frequency of the high-pass filter. Note that (3) has integral action and is unstable at DC.

4. LOW-FREQUENCY BYPASS

The simplest solution to the high-pass characteristic of the piezoelectric sensor is to make the cut-off frequency as low as possible, however, this results in an increase in settling time which becomes impractical. A low frequency bypass technique was introduced by (Yong et al., 2011) to deal with the high-pass limitations. In the proposed technique, complimentary filters are used to estimate the low frequency component of the displacement from the input voltage u. As illustrated in Fig. 6, the complimentary filters F_H and F_L were added to the closed loop system after the sensor's high-pass filter F_{HP}. As a result, an

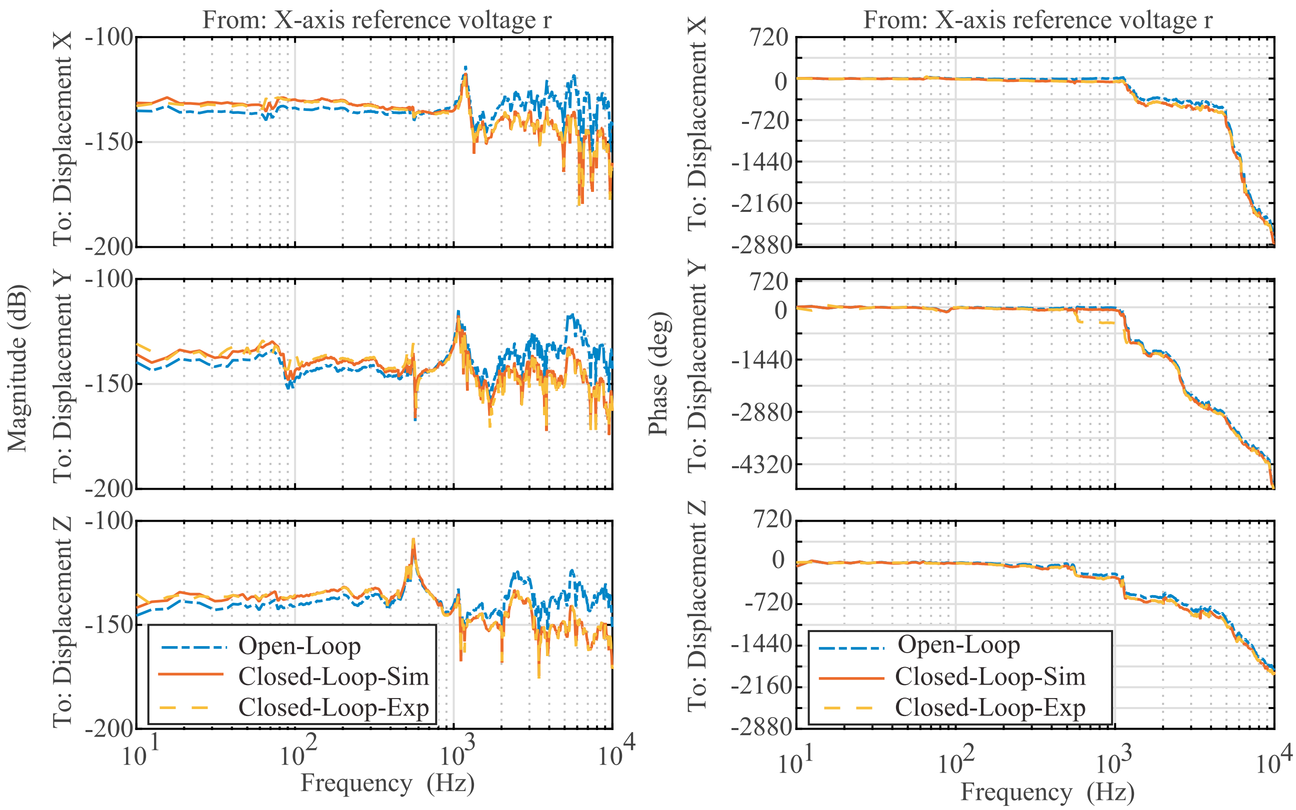

Fig. 5. The measured open-loop and the measure and simulated closed-loop frequency responses of the stage in X-axis from input r to displacement d_x, and the cross coupling responses from r to d_y and d_z, represented in a MIMO structure as $G = [G_{d_x r}; G_{d_y r}; G_{d_z r}]^T$

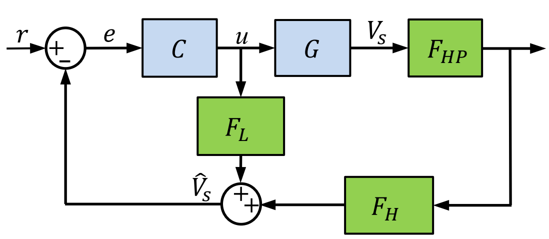

Fig. 6. The block diagram of the low frequency bypass technique proposed in (Yong et al., 2011)

additional pole is introduced in the measurement path which results in an error in the estimated voltage $\widehat{V}_s$. The effect of the second pole on the the complimentary filters is plotted in Fig. 7 where the pole of F_{HP} at 0.1 Hz causes a drop in magnitude at a rate of -40dB/decade. The error can be minimized by making the cut-off frequency of F_{HP} very low, however the associated long settling times are undesirable. Additionally, the cut-off frequency of F_{HP} moves as the capacitance of the sensor changes with temperature.

To avoid the above difficulties, the capacitance of the piezoelectric sensor can be as a component in the complimentary filters as shown in Fig. 8. This ensures identical cut-off frequencies for the high- and low-pass filters regardless of capacitance. The block diagram of this technique is shown in Fig. 9. The low-frequency component of the sensor voltage V_s is estimated from the control signal u

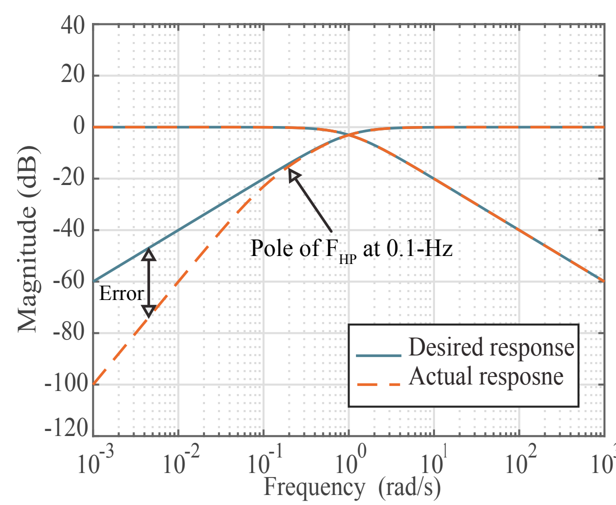

Fig. 7. The effect of additional pole on complimentary filters and the corresponding error

which is first scaled with β and passed through the filter F_{LP},

$$F_{LP} = \frac{v_s}{u} = \frac{\omega_c}{s + \omega_c}, \tag{4}$$

where $\omega_c = 1/(R_{in}C_p)$. The gain β is used to tune the DC gain of the low-pass filter F_{LP} so it matches the DC gain of the high-pass filter F_{HP}.

The circuit diagram of this technique is shown in Fig. 8. In the first stage, the sensitivity of the low-pass filter is

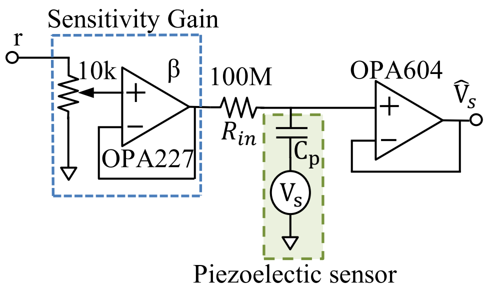

Fig. 8. Analog implementation of low-frequency bypass technique

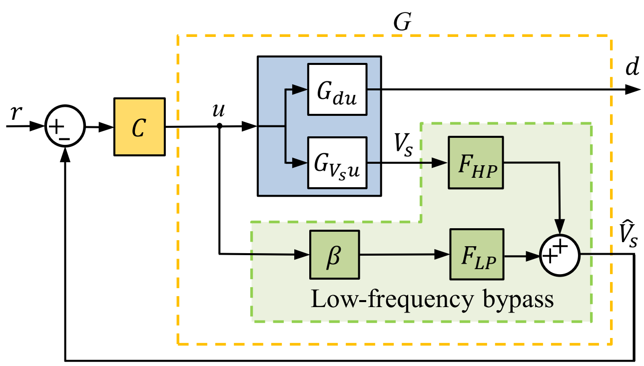

Fig. 9. The block diagram of the closed-loop system with low-frequency bypass and integral tracking control

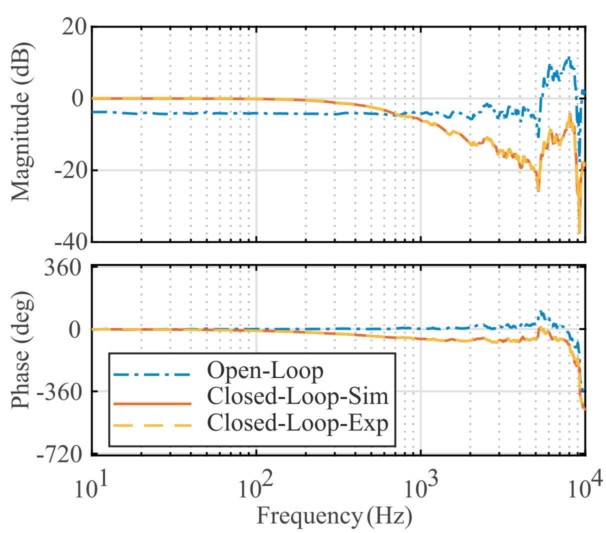

Fig. 10. The measured and simulated frequency responses from the reference input r to the sensor voltage V_s.

adjusted to match the high-pass part by the gain β and in the second stage, cut-off frequency of complimentary filters are adjusted to 0.15 Hz by the 100 MΩ input impedance.

The open-loop frequency response from the reference input r to sensor output $\widehat{V}_s$ is plotted in Fig. 10 which shows a relatively constant response for frequencies up to 2 kHz. This makes the sensor output ideal for tracking control applications.

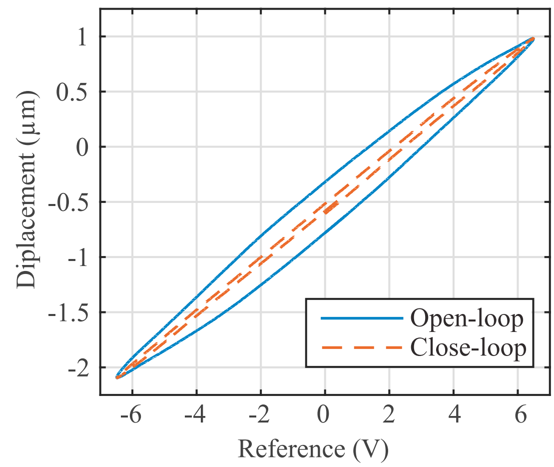

Fig. 11. Open-loop and closed-loop hysteresis exhibited by nanopositioning stage.

Triangular Reference	$e_{max}(\%)$	$e_{rms}(\%)$
5 Hz	0.54	0.24
10 Hz	0.55	0.26
15 Hz	0.51	0.26

Table 1. Comparison of rms and maximum tracking errors for different triangular frequencies

5. TRACKING CONTROL

The nanopositioning system is considered to be a single-input multi-output (SIMO) system where the input is the actuation voltage v_x and two outputs are the estimated sensor voltage $\widehat{V}_s$ and displacement d. This system can be expressed as,

$$G = \begin{bmatrix} d \\ \widehat{V}_s \end{bmatrix} u, \quad where, \quad d = \begin{bmatrix} d_x \\ d_y \\ d_z \end{bmatrix}$$

The transfer function of the system from reference r to sensor voltage $\widehat{V}_s$ is,

$$G_{\widehat{V}_s r} = \frac{\widehat{V}_s}{r} = \frac{C(F_{HP}G_{V_s u} + F_{LP})}{1 + C(F_{HP}G_{V_s u} + F_{LP})}, \quad (5)$$

where $C = k_i/s$ is an integral controller. The experimental frequency response of $G_{\widehat{V}_s r}$ in open-loop and the measured and simulated response in closed-loop is plotted in Fig. 10. The tracking bandwidth of the closed-loop system is 573 Hz with an integral gain of $k_i = 2000$. The gain and phase margins are 8.15 dB and 177° respectively.

The transfer function of the system from input r to displacement d is,

$$G_{dr} = \frac{d}{r} = \frac{G_{du}C}{1 + C(F_{HP}G_{\widehat{V}_s u} + F_{LP})}, \quad (6)$$

The experimental frequency response of G_{dr} in open-loop and the measured and simulated responses in closed-loop are plotted in Fig. 5. This plot shows the effect of the integral controller on all three axes. The first vertical mode is at 553 Hz which is the primary limitation on position bandwidth.

Fig. 11 shows the hysteresis exhibited by the nanopositioner in open- and closed-loop when the stage is driven

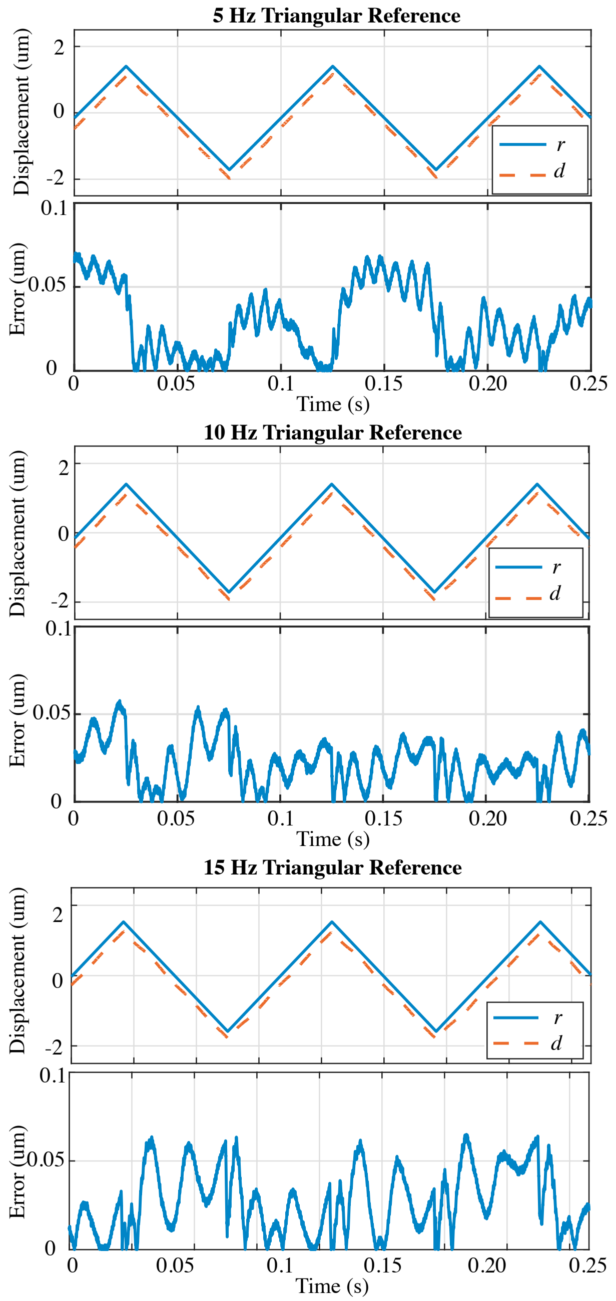

Fig. 12. Closed-loop tracking performances of the nanopositoning stage with a full-range triangular reference at 5Hz, 10Hz and 15Hz.

at full range with a 5 Hz sinusoidal reference. The results shows an 84.2 % linearity improvement in closed-loop.

The closed-loop tracking performance is plotted in Fig. 12. The root-mean square(rms) and maximum tracking error are summarized in Table.1. The tracking performance for all three frequencies are comparable as the majority of the triangular harmonics falls within the tracking bandwidth of 573 Hz.

6. CONCLUSION

In this work, a low-frequency bypass technique is introduced to deal with the high-pass characteristic of piezoelectric sensors. The capacitance of the sensor is used as a circuit component in a complimentary filter. This ensures that the complimentary filters are matched regardless of capacitance.

The proposed method is demonstrated on a monolithic piezoelectric nanopositioning stage where a set of flexures are used as sensors. The closed-loop linearity is improved by 84.2% and the the tracking error is reduced to 0.24% RMS with a 5-Hz triangular signal.

REFERENCES

Abramovitch, D.Y., Andersson, S.B., Pao, L.Y., and Schitter, G. (2007). A tutorial on the mechanisms, dynamics, and control of atomic force microscopes. In *2007 American Control Conference*, 3488–3502. IEEE.

Fleming, A.J., Berriman, G., and Yong, Y.K. (2016). Design, modeling, and characterization of an xy nanopositioning stage constructed from a single sheet of piezoelectric material. In *IEEE Advanced Intelligent Mechatronics*. Banff, Canada.

Fleming, A.J. (2010). Nanopositioning system with force feedback for high-performance tracking and vibration control. *IEEE/Asme Transactions on Mechatronics*, 15(3), 433–447.

Fleming, A.J. and Leang, K.K. (2010). Integrated strain and force feedback for high-performance control of piezoelectric actuators. *Sensors and Actuators A: Physical*, 161(1), 256–265.

Fleming, A.J. and Leang, K.K. (2014). *Design, modeling and control of nanopositioning systems*. Springer.

Hassen, S.S., Heurs, M., Huntington, E., Petersen, I.R., and James, M. (2009). Frequency locking of an optical cavity using linear–quadratic gaussian integral control. *Journal of Physics B: Atomic, Molecular and Optical Physics*, 42(17), 175501.

Kuiper, S. and Schitter, G. (2010). Active damping of a piezoelectric tube scanner using self-sensing piezo actuation. *Mechatronics*, 20(6), 656–665.

Mishra, S., Coaplen, J., and Tomizuka, M. (2007). Precision positioning of wafer scanners segmented iterative learning control for nonrepetitive disturbances [applications of control]. *IEEE control systems*, 27(4), 20–25.

Salapaka, S.M. and Salapaka, M.V. (2008). Scanning probe microscopy. *IEEE Control Systems*, 28(2), 65–83.

Sebastian, A., Pantazi, A., Pozidis, H., and Eleftheriou, E. (2008). Nanopositioning for probe-based data storage [applications of control]. *IEEE Control Systems*, 28(4), 26–35.

Sirohi, J. and Chopra, I. (2000). Fundamental understanding of piezoelectric strain sensors. *Journal of Intelligent Material Systems and Structures*, 11(4), 246–257.

Yong, Y.K., Fleming, A.J., and Moheimani, S.O.R. (2011). Vibration and tracking control of a flexure-guided nanopositioner using a piezoelectric strain sensor (invited paper). In *Proc. International Conference on Manipulation, Manufacturing and Measurement on the Nanoscale*. Changchun, China.

Yong, Y.K., Fleming, A.J., and Moheimani, S. (2013). A novel piezoelectric strain sensor for simultaneous damping and tracking control of a high-speed nanopositioner. *IEEE/ASME Transactions on Mechatronics*, 18(3), 1113–1121.